Irreducible Fluid Saturation Determined by Pulsed Field Gradient NMR

F. Stallmach[1], M. Appel, and H. Thomann*

Exxon Corporate Research
Route 22 East, Annandale, NJ 08801

Abstract

A new laboratory procedure, using a pulsed field gradient (PFG) NMR technique, for measuring the relative volumes of movable and non-movable fluid in cores is reported. The saturations determined are in qualitative agreement with values obtained from mercury porosimetry and centrifuged gravimetric saturation measurements. An advantage of the PFG NMR method is that it is fast and does not require exchange of fluids, i.e., progressive desaturation. This may be important if wettability changes are a concern or for measurements on unconsolidated cores. The BVI of some core plugs was additionally determined by CPMG NMR which was recently established as a down-hole measurement with the new generation of NMR well logging tools. Since PFG NMR is not sensitive to surface relaxivity, this technique can be used as a quick and independent check on the BVI values obtained by CPMG NMR.

[1] Present address: SINTEF Unimed, Plav Kyrres gt. 3, N-7034 Trondheim, Norway
* Author to whom correspondence should be addressed.

Introduction

As a qualitative measure of producibility, the total pore volume of a reservoir rock is considered to be comprised of movable and non-movable fluid volumes. When expressed as a fraction of the pore volume, the movable fluid volume is often referred to as the Free Fluid Index, FFI, while the non-movable fluid volume is known as the Bound Volume Index, BVI. The FFI and BVI are typically used in formation evaluation as an indication of the economic potential of a reservoir. The standard petrophysical method to determine the FFI and BVI in laboratory measurements on reservoir core plugs is to determine the capillary pressure curve by progressive centrifuge desaturation of the core plug. The BVI is the fluid volume remaining at a pre-selected capillary pressure, as determined by the centrifugation conditions. Alternatively, the BVI can be determined from mercury porosimetry, after corrections for the wettability are taken into account.

A recent addition to the methods for determining the FFI and BVI is the NMR CPMG experiment./1,2/ A distinctly attractive feature of these measurements is that they can be performed on both bench-top NMR instruments and down-hole using the new generation of NMR well logging tools./3/ In the NMR measurement, the core plug is placed in a magnetic field and a long string of radio frequency pulses is applied. Each of the pulses is separated by a pre-defined time interval known as the echo time, or TE. The signal observed, known as a spin echo signal, is the nuclear magnetization, and is detected at time intervals TE after the first echo. The observed signal only arises from the fluids in the pore space.

For fluid in a single, isolated pore, and for the condition known as the fast diffusion limit /4/, the magnetization, $m(t)$, is a simple exponential:

$$(1) \qquad m(t) = m_0 \exp(-t / T_2)$$

The time constant, T_2, known as the transverse relaxation time, is related to the pore surface to volume ratio, S/V, by: /4/

$$(2) \qquad T_2^{-1} = \rho \frac{S}{V}$$

The constant, ρ, which has dimensions of velocity, is known as the surface relaxation velocity or surface relaxivity, connects the length scale of the rock pore space to the decay time for the fluid magnetization in the NMR measurement. Thus, to preserve this simple relationship between the measured decay time constant and a pore length, ρ must not be variable from pore to pore. Once a pore length r is determined from the measured NMR relaxation time, a capillary pressure can be calculated using the Young-Laplace equation:

$$(3) \qquad p_c = 2 \gamma r^{-1} \cos\theta$$

where γ is the interfacial energy and θ is the contact angle.

Since rocks are comprised of a pore size distribution, the observed magnetization decay in the CPMG NMR experiment is a multi-exponential:

$$(4) \qquad M(t) = \sum_i m_i^0 \exp(-t / T_{2,i})$$

A distribution of T_2 values can, in principle, be obtained by a non-linear least squares fit of a multi-exponential function to the experimental data. Alternatively, the time domain data can be "inverted" to a "T_2 domain" display in which the amplitude for a given T_2 is displayed. In either case, the uniqueness of the solution is not guaranteed since several T2 distributions can give the same magnetization decay in the time domain.

Once the T_2 distribution has been obtained, a T_2 cut-off is used to differentiate the FFI and BVI fluid volumes. The BVI value is the integrated signal from the lowest T_2 value (typically 1 msec) to the T_2 cut-off value. Based on CPMG NMR data collected for a very large number of sandstone samples, it has been proposed that a T_2 cut-off of 33 msec can be universally applied (to clastic rocks) for estimating BVI./1,2/ The FFI value is the integrated signal from the T_2 cut-off to the longest T_2 value observed.

There are several complications to this simple model that must be considered to adequately describe the NMR relaxation data on rocks. First, the surface relaxivity is generally an unknown parameter. The rock mineralogy, surface chemistry, and surface roughness can all affect ρ. Thus, if a standard rock is used to calibrate ρ, the unknown rock must be similar to the standard with respect to these properties. Second, the model assumes that the rock pores are isolated. Diffusion of fluid molecules between pores during the NMR relaxation measurement changes the S/V and therefore shifts the observed T_2. For a pore size distribution, the overall shape of the T_2 distribution will be affected since T_2 lines will be narrowed by variable amounts. Third, the effects of different pore geometries, e.g., spherical vs cylindrical vs sheet, will also affect the simple relation between relaxation time and pore length. Taken together, these complications have the consequence that a single T_2 cut-off time may not be adequate for determining the BVI and FFI values from the CPMG NMR experiment.

Another approach for determining the BVI and FFI in rocks is to measure the pore size directly using the Pulsed Field Gradient (PFG) NMR experiment. The PFG NMR experiment is a well established method for measuring the mean square displacement of fluid molecules./5,6,7/ The Stokes-Einstein relation for Brownian motion connects the z-coordinate, which is the measured direction of displacement, to the fluid diffusivity:

$$(5) \qquad \left\langle z^2(\Delta) \right\rangle = 2 D_0 \Delta$$

where D_0 is the molecular diffusivity. The pulsed magnetic field gradients encode the molecular displacements to be observed as a reduction in the amplitude of the observed spin echo signal. The echo reduction factor, ψ, is the ratio of the echo in the presence and absence of the pulsed magnetic field gradients:

$$(6) \qquad \psi = \exp(-(\gamma \delta g)^2 D_0 \Delta)$$

where Δ is the diffusion time, i.e., the time during which the molecular displacements are observed, g is the amplitude of the magnetic field gradient pulse, δ is the duration or width of the magnetic field gradient pulse, and γ is the magnetogyric ratio (a constant for a given nucleus which specifies the NMR frequency for a given magnetic field). Note that the product ($\gamma\delta g$) has dimensions of inverse length and, since the magnetic field gradient is a vector quantity, can be described as a wave vector. The wave vector construct is useful to identify the length scale over which the molecular displacements can be measured in the experiment. Recently it has been shown that the shape of the echo attenuation curve can under certain conditions directly provide structural information about a porous medium./8,9/

Eq. (6) is valid in the limit of free diffusion, which requires that the diffusing molecules do not encounter restrictions to their displacements. Fluid molecules in the pore space of rocks must encounter the pore wall as the diffusion time increases. Once this wall collision occurs, the mean square displacement is no longer a linear function of time defined by the Stokes-Einstein relation, eq. (5). This phenomena is known as restricted diffusion.

One manifestation of restricted diffusion is that the self-diffusivity in the Stokes-Einstein relation becomes time dependent:

$$\left\langle z^2(\Delta)\right\rangle = 2D_{app}(\Delta)\Delta \tag{7}$$

where $D_{app}(\Delta)$ is time dependent and is known as the apparent diffusivity. For small diffusion times, Δ, $D_{app}(\Delta)$ is equal to the self-diffusivity of the bulk fluid in eq. (5). With increasing diffusion time, an ever increasing number of fluid molecules experience collisions with the pore walls. Consequently, the mean square displacement, $\left\langle z^2(\Delta)\right\rangle$, increases less rapidly than in the case of free, i.e., unrestricted, diffusion and $D_{app}(\Delta)$ decreases with increasing diffusion time.

For fluid in well connected rock pores and at very long diffusion times, $D_{app}(\Delta)$ approaches a time independent value which is known as the long range self-diffusivity, $D_{l.r.}$, given by:

$$D_{app}(\Delta \rightarrow \infty) = D_{l.r.} = D_0 / \tau \tag{8}$$

where τ is known as the tortuosity factor. This long range diffusion time regime is identified by a new linear dependence of the mean square displacement on the diffusion time:

$$\left\langle z^2(\Delta \rightarrow \infty)\right\rangle = 2\, D_{l.r.}\, \Delta \tag{9}$$

Such anomalous diffusion has recently been observed for fluids in a host matrix of polypropylene./10/

In principle, the mean square displacement in such well connected pores has no upper bound. In practice, the upper bound for observing the NMR signal is $\Delta \approx 3T_{1n}$ (T_{1n} is the nuclear spin lattice relaxation time).

For water at room temperature, T_{1n} is on the order of 1 to 3 sec. In rocks, this value is reduced by collision of the water molecules with the pore wall, in analogy to eq. (2). Thus, the tortuosity and effective spin-lattice relaxation time will determine whether the long range diffusivity is observed.

For fluid in poorly connected rock pores, the upper bound of the mean square displacement is limited by the size of the pores. At long diffusion times, the mean square displacement becomes much larger than the pore size. This requires that many wall collisions have occurred which implies that the mean square displacement approaches a constant value at sufficiently long diffusion times. For a spherical pore of radius R, the echo attenuation for long diffusion times is given by: /11/

$$(10) \qquad \psi = \frac{9(\gamma \delta g R \cos(\gamma \delta g R) - \sin(\gamma \delta g R))^2}{(\gamma \delta g R)^6}$$

For values $\gamma \delta g R \leq 1$, i.e. if the length scale measured in the experiment is greater than the radius of the pore, eq. (10) reduces to:

$$(11) \qquad \psi = \exp(-(\gamma \delta g)^2 R^2 / 5)$$

Comparing the equation for describing the echo attenuation in the case of restricted diffusion (eq. (11)) to the expression valid for free diffusion (eq. (6)) yields the apparent self-diffusivity in a spherical pore:

$$(12) \qquad D_{app}^{sphere}(\Delta \rightarrow \infty) = R^2 / (5\Delta)$$

According to eq. (12), the apparent self-diffusivity in such a spherical pore is inversely proportional to the diffusion time. Thus, diffusion measurements in small poorly connected pores may yield very small apparent self-diffusivities at long diffusion times. Furthermore, the apparent diffusivities are independent of the true self-diffusivity D_0 of the fluid.

The mean square displacement of the molecules confined in a spherical pore can be calculated using the Stokes-Einstein relation (eq. (7)) and the apparent self-diffusivity according to eq. (12):

$$(13) \qquad \left\langle z^2(\Delta \rightarrow \infty) \right\rangle_{sphere} = 2R^2 / 5$$

Note that the mean square displacement becomes time independent but is only determined by the size of the pore. Similar relations such as eqs. (12) and (13) exist for other simple restricting geometries.

The cross-over from free to restricted diffusion and between different regimes of restricted diffusion can be used to determine the pores size of a porous material. Since the individual diffusion regimes have significantly different diffusion time dependencies of the mean square displacements (see eqs. (5), (7), (9), (13)), PFG NMR measurements of $\langle z^2 \rangle$ as a function of Δ provides, in principle, a unique approach for characterizing the pore system. However, since a range of pore sizes are encountered in rocks, it is anticipated that there will be a corresponding range of cross-over times from free to restricted diffusion. This significantly complicates the PFG NMR data analysis.

The exact functional forms, i.e., the time dependence of $D(\Delta)$ in eqs. (7) and (9) are not known for arbitrary geometries of pores that can be encountered in rocks. A first order correction for relating the measured diffusivity to the true diffusivity has been published. /12/ While the theory is independent of the pore microgeometry, it is only valid for very short diffusion times and small gradient wave vectors for which only a small departure from the linearity of the Stokes-Einstein relation, eq. (5), is expected and the echo attenuation reduction factor can be approximated by the simple exponential function of eq. (6). Thus the theory can not account for the strong departure from single exponential behaviour for large gradient wave vector values observed over a large range of diffusion times.

Below we demonstrate that a simple bi-exponential model fits the PFG NMR data for all accessible diffusion times, even at high gradient wave vector values. The microscopic origin of these two exponential components is revealed from the time dependence of the mean square displacements corresponding to the respective diffusivities.
Furthermore, BVI values can be predicted from this simple phenomenological model which are in qualitative agreement with the BVI values derived from both mercury porosimetry and standard capillary pressure data.

Experimental Considerations

Core Preparation: Sandstone core plugs of about 2 cm length and 1 cm diameter were prepared by first evacuation to roughly 0.2 Torr and then imbibing with distilled water. The cores were stored immersed in water in sealed containers. In order to prevent drainage of water in high permeability cores during the NMR measurements, the cores were sealed in Teflon tape and then transferred into NMR tubes. The porosities and permeabilities for the sandstone core plugs included in the current study are summarized in Table I.

NMR Experiments: A Bruker Instruments MSL-300 spectrometer equipped with imaging accessory was used to collect data at a magnetic field of 7.05 Tesla. A TECHRON 7570 amplifier was used to produce the constant current pulses necessary to drive the magnetic field gradient pulses in the B_0-direction. A diffusion probe with actively shielded gradient coils designed by Doty Scientific Inc. was used. Magnetic field gradient strengths (i.e., g) of up to 1T/m were used. NMR measurements were also performed on a low magnetic field bench top NMR manufactured by Resonance Instruments, model Maran-2. Homemade modifications were made to the NMR probe and to the operating software.

The timing diagram for the rf and magnetic field gradient pulses are shown in Fig. 1. PFG NMR diffusion measurements at high magnetic field were performed using a slight modification, shown in Fig. 1b, of the 17-interval-condition I sequence suggested by Cotts /14/. This pulse sequence for the rf and magnetic field gradient pulses offers the advantage of cancellation of cross terms between the applied pulsed field gradients and the internal field gradients in the rock sample. The latter arise from the magnetic susceptibility difference between the rock grain material and the fluid in the pore space. If these cross terms are not canceled, the echo attenuation will not be a simple exponential even when the free diffusion condition applies. The bi-polar magnetic field gradient pulses are not required for PFG NMR measurements performed at low magnetic field since the internal magnetic field gradients are proportional to the applied magnetic field while the applied magnetic field gradient pulses are of course independent of the static magnetic field. The cross terms of these magnetic fields are therefore small and the more simple stimulated echo sequence, shown in Fig. 1a, is adequate.

In order to assist the matching of the pulsed field gradients, a pair of bipolar pulsed field gradients was added prior the initial rf excitation . Pulsed field gradient intensities were calibrated by measuring the echo attenuation of bulk water with this pulse sequence at different observation times. The corresponding spin echo attenuation was observed to be a simple exponential when plotted against the square of the applied gradient current over three orders of magnitude of the attenuation.

For the 17-interval sequence, the observation time in eq. (6) had to be corrected by $\Delta=\Delta'-\delta/3-T/2$ /12/, were Δ' is the time between the on-set of magnetic field gradient pulses of equal polarity, δ is twice the width of a single field gradient pulse and T is the time between the on-set of gradient pulses of opposite polarity in a single pair of bipolar field gradient pulses. δ and T were chosen to be constant for all Δ and g values used to measure the water diffusion in one particular rock. T was always equal to $\delta/2+1.1$ms. δ was chosen to be between 1.414 ms and 4 ms. Spin echo attenuations were measured by stepping linearly through the gradient intensity g.

CPMG NMR measurements were made at both low and high magnetic fields. The high field measurements were carried out as described in ref. /15/. The transverse magnetization was sampled at the time TE/2 after each π rf pulse. TE was chosen to be 1 ms. 1k of data points was acquired for each core plug.

Results

Representative PFG NMR data, recorded for a Marsing sandstone is shown in Fig. 2. The echo attenuations were recorded as a function of gradient wave vector values, i.e., ($\gamma\delta g$), and for a variety of diffusion time values. Only a few of all measured diffusion time values are shown in Fig. 2. According to eq. (6), for the condition of free diffusion, the logarithm of the echo attenuations decay linearly when plotted against $(\gamma\delta g)^2$. As observed in Fig. 2, the echo attenuations deviate from the linear behaviour expected for simple free diffusion for all observation times. A linear approximation is valid only for small values of $(\gamma\delta g)^2$. Note also that the echo attenuations approach a plateau value with increasing values of the gradient wave vector and appear to approach the same asymptotic value at the highest wave vector values for all diffusion times. Similar non-linear behaviour has been reported in other PFG NMR studies of fluids in rocks./16-20/

As discussed in the introduction, the presence of the pore size distribution expected in rocks significantly complicates the quantitative analysis of the PFG NMR data. Since no theory currently exists to account for the PFG NMR data recorded over the range of gradient wave vector values shown in Fig. 2, we adopt a simple phenomenological model adapted from the BVI and FFI analysis of the CPMG NMR data. Accordingly, we classify the pore size distribution into two categories. The pores contributing to the FFI are expected to be large and most likely well connected. The mobility for fluid in these pores should be in the free and weakly restricted diffusion limits. The mean square displacement determined from the PFG NMR experiment would then be time dependent as anticipated by eq. (5). In contrast, the pores contributing to the BVI should be in the strongly restricted limit. In this limit, the mean square displacement is time independent. Physically, this means that the fluid molecules make multiple collisions with the pore wall during the observation (i.e., diffusion) time. Thus, fluid in the pore space contributing to the FFI is expected to have a larger, time independent

diffusivity, D_h, while fluid in the BVI pore space should have a lower, time dependent diffusivity, D_l. We represent these two fluid "types" using a bi-exponential expression for echo attenutation:

$$(14) \quad \psi((\gamma\delta g)^2,\Delta) = p_h \cdot \exp(-(\gamma\delta g)^2 D_h \Delta) + p_l \cdot \exp(-(\gamma\delta g)^2 D_l \Delta)$$

where p_l and p_h are the fluid volumes corresponding to the BVI and FFI. Note that $p_h + p_l = 1$. Thus, there are three independent variables, D_h, D_l and p_l, that must be determined from the non-linear least squares fit to the experimental data. The model also implicitly assumes that there is no exchange of fluids, by for example diffusion, between the fluid volumes corresponding to the BVI and FFI.

The solid lines in Fig. 2 are the best fits of eq. (14) to the PFG NMR data. Note that this simple bi-exponential, or "two fluid", model fits the experimental data quite well for the full range of diffusion times, from 25 ms to 600 ms. The coefficients, p_l and p_h, determined from the PFG data recorded for a range of diffusion times are shown in Fig. 3b. According to the assumptions of the model, these coefficients correspond directly to the BVI and FFI, respectively. Note that the p_l values calculated for different diffusion times vary from 0.21 to 0.11 with the tendency to decrease with increasing observation time. This tendency can be understood if surface relaxation /21/ is assumed to be an important relaxation process. Surface relaxation is more efficient in small pores since the mean number of collisions of a water molecule with the pore wall exceeds the corresponding number in large pores, reducing the relative contribution to the spin echo amplitude from molecules in small pores with increasing Δ. Thus, for reducing the effects of surface relaxation, PFG data should be collected at short observation times. However, the diffusion times must also be sufficiently long to insure that the fluid component with low diffusivity is in the strongly restricted diffusion regime. This is indicated by the observation of the plateau value in the echo attenuation data in Fig. 2. This is in fact a more rigorous condition for the current model to apply. Thus data should be collected at sufficiently long diffusion times to ensure that a plateau value has been reached.

Discussion

In Table I, a comparison is shown between the BVI values derived from PFG NMR and low (magnetic) field CPMG NMR data, mercury porosimetry data, and capillary pressure data. Except for the rock Table #2, the BVI values obtained by PFG NMR are in good agreement with values from CPMG NMR and both agree very well with the BVI values determined by mercury porosimetry. The BVI values from these three techniques are also in reasonably good agreement with the BVI values derived by air-brine centrifugation measurements, although the other three methods tend to slightly under-estimate the air-brine data (except for Table #2). The dispersion of values (with the exception of Table #2) is not large enough to warrant extensive analysis, since the inherent differences in the measurement techniques and the intrinsic errors in each measurement can readily account for the results. The air-brine values may have larger errors relative to usual centrifugation data because of the smaller core plug size (1 cm vs 3.9 cm diameter normally used). A factor of 2 difference in BVI values could also originate from the natural variabilities in the pore level properties of the core plugs. As an example, note the range of BVI values calculated from the mercury porosimetry data obtained on the three different Marsing #1 core plugs.

The results on the Table #2 core plug are an exception to the discussion above. It is unlikely that

the natural variation of rock properties can account for the large discrepancy of BVI values derived from the four types of measurements. Whereas the mercury porosimetry and the air-brine centrifugation data of this sample are in good agreement, the BVI value determined by PFG NMR over-estimates the centrifugation value by roughly a factor 2, while CPMG under-estimates the BVI value from air-brine centrifugation by a factor of 6. This suggests that the difference in the BVI values derived from the NMR measurements most likely originates from the peculiarities intrinsic to these measurements. A analysis of the results must also take into account the over-estimation by the PFG NMR method and the under-estimation by the CPMG NMR experiment.

The main difference between the NMR methods (PFG and CPMG) and the other two techniques (air-brine centrifugation and mercury porosimetry) is that PFG NMR and CPMG NMR do not require the displacement of fluids. The NMR measurements do not directly measure volume fractions of displaced fluids, as is the case for the air-brine centrifugation measurement. Both the PFG and CPMG NMR experiments measure a pore length, the former directly from the thermally driven displacement of molecules as a function of time and the latter indirectly, by converting the measured spin relaxation time to a length using the surface relaxivity. Neither technique can unambiguously distinguish fluids in connected from isolated pores. The under-estimation of the BVI in the CPMG experiment can be explained by a longer surface relaxivity due to a low amount of paramagnetic impurities in the rock. According to eq. (2), a longer surface relaxivity shifts the determined relaxation time distribution to larger values of T_2, thus leading to an under-estimation of the BVI if the universally used value of 33 msec is applied to determine the T_2 cut-off. To obtain a BVI value of about 7 % for the rock Table #2, a T_2 cut-off of about 65 msec must be used.
In contrast to this, PFG NMR is not sensitive to surface relaxivity. This technique determines the volume fraction of fluid in any pore if the pore length is experimentally accessible by the applied wave vector, i.e. strength of the magnetic field gradient. The pores need not be connected to be measured by PFG NMR. Therefore, this method over-estimates the BVI values determined by air-brine centrifugation and mercury porosimetry with the volume fraction of isolated and poorly connected pores that are invisible for measurements requiring the displacement of fluids. The difference of the BVI values for the sample Table #2 can be explained by assuming a relatively large amount of poorly connected pores with a weak surface relaxivity.

The analysis of the experimental spin echo attenuation data yields the self diffusion coefficients $D_{h(l)}$ and the fluid volume fractions $p_{h(l)}$ of water molecules with high and low translational mobility, respectively. According to eq. (7), the observation time dependence of the mean square displacement for both fluid fractions may be calculated. The results for water in the Marsing sandstone are shown in Fig. 3a. For comparison the time dependence of the mean square displacement for bulk water is also shown in the figure. The mean square displacement of water with high translational mobility is found to increase over the whole range of observation times. However, this increase is non-linear and slower than for bulk water. Clear deviations from the mobility of bulk water occur for observation times $\Delta >$ 50ms, indicating a cross-over from free to restricted diffusion. Using the room temperature diffusivity of water, this diffusion time corresponds to a root mean square displacement of about 15 µm. This length sets a lower limit for the radius of pores containing the fluid with high translational mobility.

The mean square displacement of water with low translational mobility is on the order of 5 μm^2 for the Marsing sandstone. Significantly, the displacement is independent of diffusion time, indicating

that the diffusion is restricted even for short observation times. The mean square displacement is therefore limited by the maximum size of the pores containing the low mobility fluid fraction. Applying eq. (13) yields a maximum pore radius of 7.9 μm for the pore in which the fluid with low translational mobility is contained. The capillary pressure for these pores can then be calculated from the Young-Laplace equation using this pore size. The capillary pressure is in the range of 50 to 100 psi depending on the choice of reasonable contact angles and interfacial energy.

Summary

A new laboratory procedure, using a pulsed field gradient (PFG) NMR technique, for measuring the movable and non-movable fluid volumes in cores is reported. Good agreement is observed between the BVI values determined from the PFG NMR experiment and values determined from air-brine centrifugation, mercury porosimetry, and CPMG NMR. The primary advantage of the PFG NMR (or CPMG measurements) are that they are quick, do not require the exchange or displacement of fluid volumes, and (in contrast to mercury porosimetry) the measurements are non-destructive.

Acknowledgements: We thank M. Bernardo for invaluable technical assistance in the PFG and CPMG NMR measurements, J. Shafer for measuring the capillary pressure data and A. Guzman-Garcia for assistance in processing the CPMG data.

References

1 M.N. Miller et al., paper SPE 20561 presented at the 65th Annual Technical Conference and Exhibition of the Society of Petroleum Engineers, New Orleans, Sept. 23-26, 1990.

2 C. Straley, C.E. Morriss, W.E. Kenyon and J.J. Howard, in "32nd Annual Logging Symposium", Transactions: SPWLA, June 1991, paper CC 1

3 NUMAR Corp.; Schlumberger Corp.; Western-Atlas Corp.

4 M.H. Cohen and K.S. Mendelson, J. Appl. Phys. **53**, 1127 (1982).

5 E.O. Stejskal and J.E. Tanner, J. Chem. Phys. **42**, 288 (1965)

6 P.T. Callaghan, "Principles of Nuclear Magnetic Resonance Microscopy", Clarendon, Oxford, 1991

7 J. Kärger, H. Pfeifer and W. Heink, Adv. Magn. Reson. **12**, 1 (1988)

8 D.G. Corey and A.N. Garroway, Magn. Resonance Medicine **14**, 435 (1990)

9 P.T. Callaghan, A. Coy, D. MacGowan, K.J. Packer and F.O. Zelaya, Nature **351,** 467 (1991)

10 M. Appel, G. Fleischer, J. Kaerger, F. Fujara, and S. Siegel, Europhys. Lett. **34**, 483 (1996).

11 J.E. Tanner and E.O. Stejskal, J. Chem. Phys. **48**, 1768 (1968)

12 P.P. Mitra and P.N. Sen, Phys. Rev. B **45**, 143 (1992)

13 P.P. Mitra, P.N. Sen, L.M. Schwartz and P. Le Doussall, Phys. Rev. Lett. **68,** 3555 (1992)

14 R.M. Cotts, M.J.R. Hoch, T. Sun and J.T. Markert, J. Magn. Reson. **83**, 252(1989)

15 M. Jerosch-Herold, H. Thomann, A.H. Thompson, Magn. Reson. Imaging **12**(2), 249 (1994)

16 P.S. Sen and M.D. Hurlimann, J. Chem. Phys. **101**, 5423 (1994).

17 L.L. Latour, L. Li and C. H. Sotak, J. Magn. Reson. B **101**, 72 (1993)

18 A. J. Lucas, S.J. Gibbs, M. Peyron, G.K. Pierens, L.D. Hall, R.C. Stewart and D.W. Phelps, Magn. Reson. Imaging **12**(2), 249 (1994)

19 E.J. Fordham, S.J. Gibbs and L.D. Hall, Magn. Reson. Imaging **12**(2), 279 (1994)

20 P.N. Tutunjian, H.J. Vinegar, J.A. Ferris and G.J. Nesbitt, in "34th Annual Logging Symposium", Transactions: SPWLA, June 1993, paper II 1

21 R.L. Kleinberg and M.A. Horsfield, J. Magn. Reson. **88**, 9 (1990)

Table I: Comparison of the bound fluid index as a % of total porosity determined by different methods for water in rocks

Rock	Porosity	Perm.	Air-Brine Centrifugation 50 psi eq.	Hg Pc 50 psi eq.	CPMG Core Labs	PFG NMR
	(He %)	mD	BVI (%)	BVI (%)	BVI (%)	BVI (%)
Nugget	10.9	4		28		25 +/- 5
Silver #1	12.2	14		58, 78 *		88 +/- 2
Layerd Navajo	25.1	883				5 +/- 1
Red Navajo	23.6	1138	8	6	5.3	5 +/- 1
Marsing #1	23.9	1276	24	9, 11, 19 *	17.5	15 +/- 5
Table #2	24.1	3000	8	7	1.3	20 +/- 10
Silver #2	30.1	21000	15	6	7.6	8 +/- 2
Marsing #2	29.5	54000		4,7 *		4 +/- 1
				* different cores		

Figure Captions

Fig. 1: Timing diagram for the radio frequency and magnetic field gradient pulses. The pulse sequence in (a) is used for experiments performed at low magnetic fields. The sequence in (b) is used at high magnetic fields.

Fig. 2: Echo attenutation pulse field gradient NMR data for a marsing sandstone from the Boise sandstone formation.

Fig. 3: (a) Mean square displacement as a function of diffusion time for the Marsing sandstone. (b) Relative fluid volume fractions for the FFI (high mobility) and BVI (low mobility) fluid components determined from the PFG NMR data analysis for data collected for variable diffusion times.

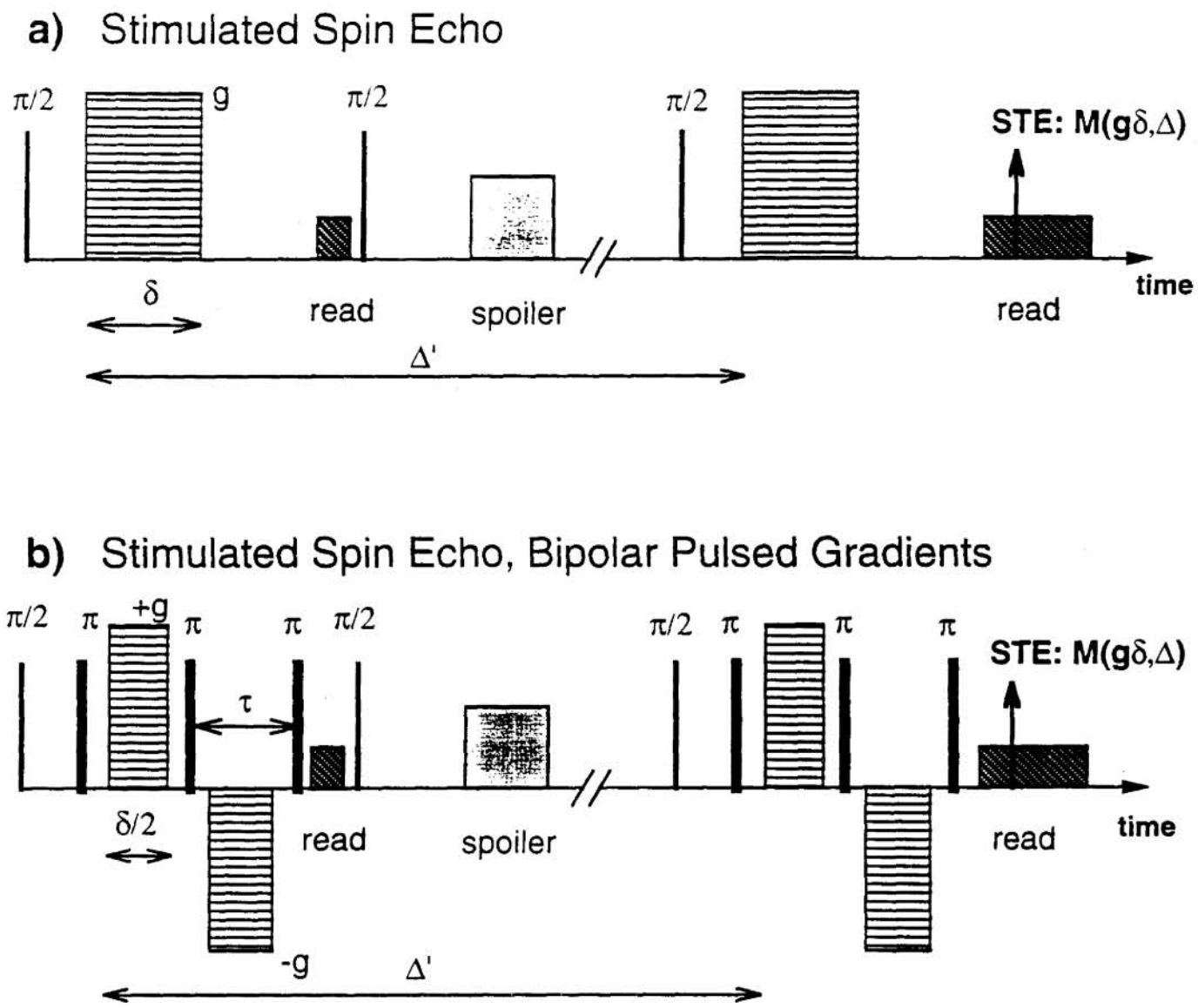
a) Stimulated Spin Echo
π/2
g
π/2
π/2
STE: M(gδ,Δ)
time
δ
read
spoiler
read
Δ'
b) Stimulated Spin Echo, Bipolar Pulsed Gradients
π/2
π
+g
π
π
π/2
π/2
π
π
π
STE: M(gδ,Δ)
τ
δ/2
read
spoiler
read
time
-g
Δ'
Magnetic field gradients:
pulsed gradient
diffusion encoding
read gradient
spoiler gradient

Fig. 1

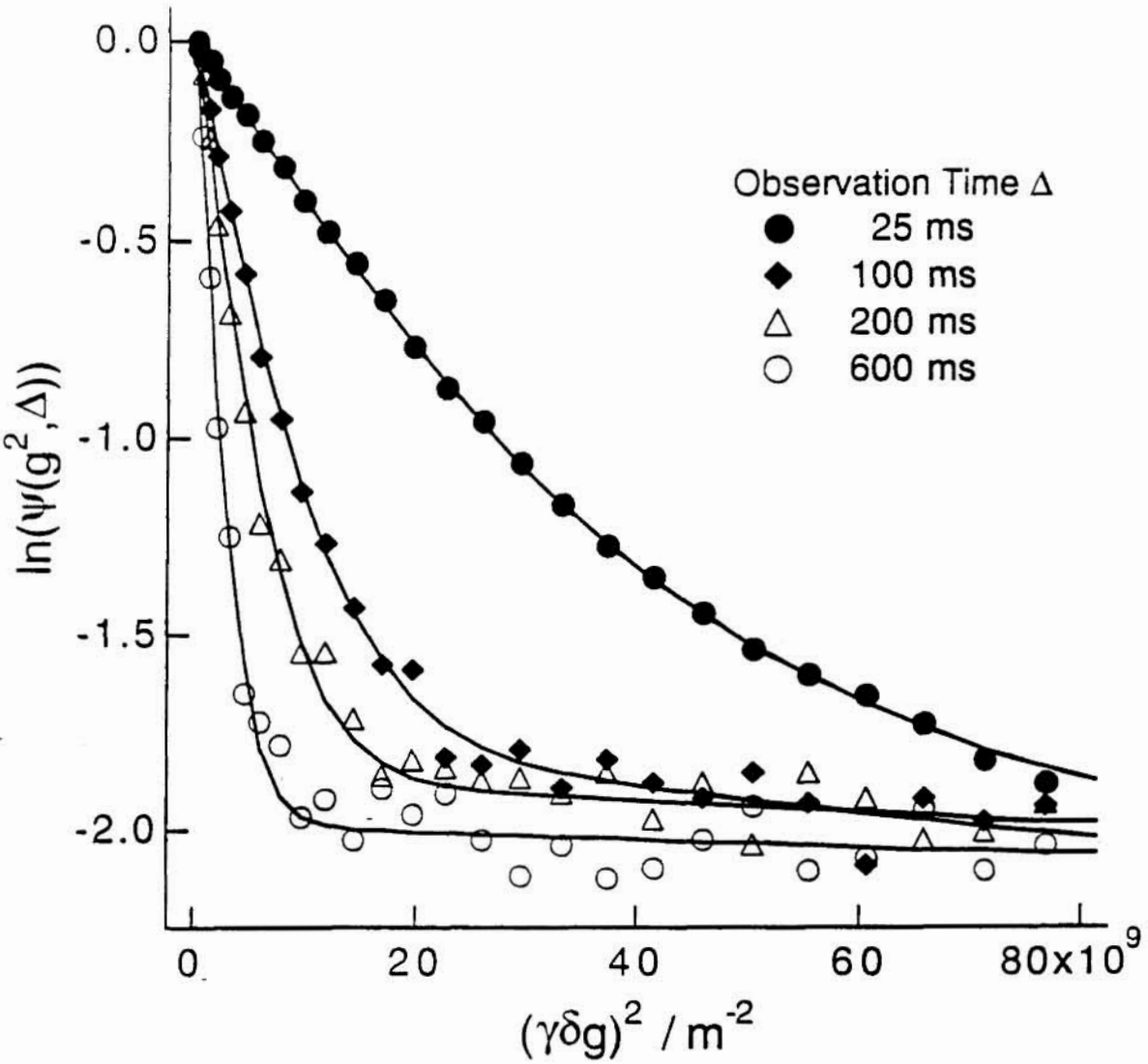
0.0
-0.5
-1.0
-1.5
-2.0
ln(ψ(g²,Δ))
Observation Time Δ
25 ms
100 ms
200 ms
600 ms
0
20
40
60
80x10⁹
(γδg)² / m⁻²

Fig.2

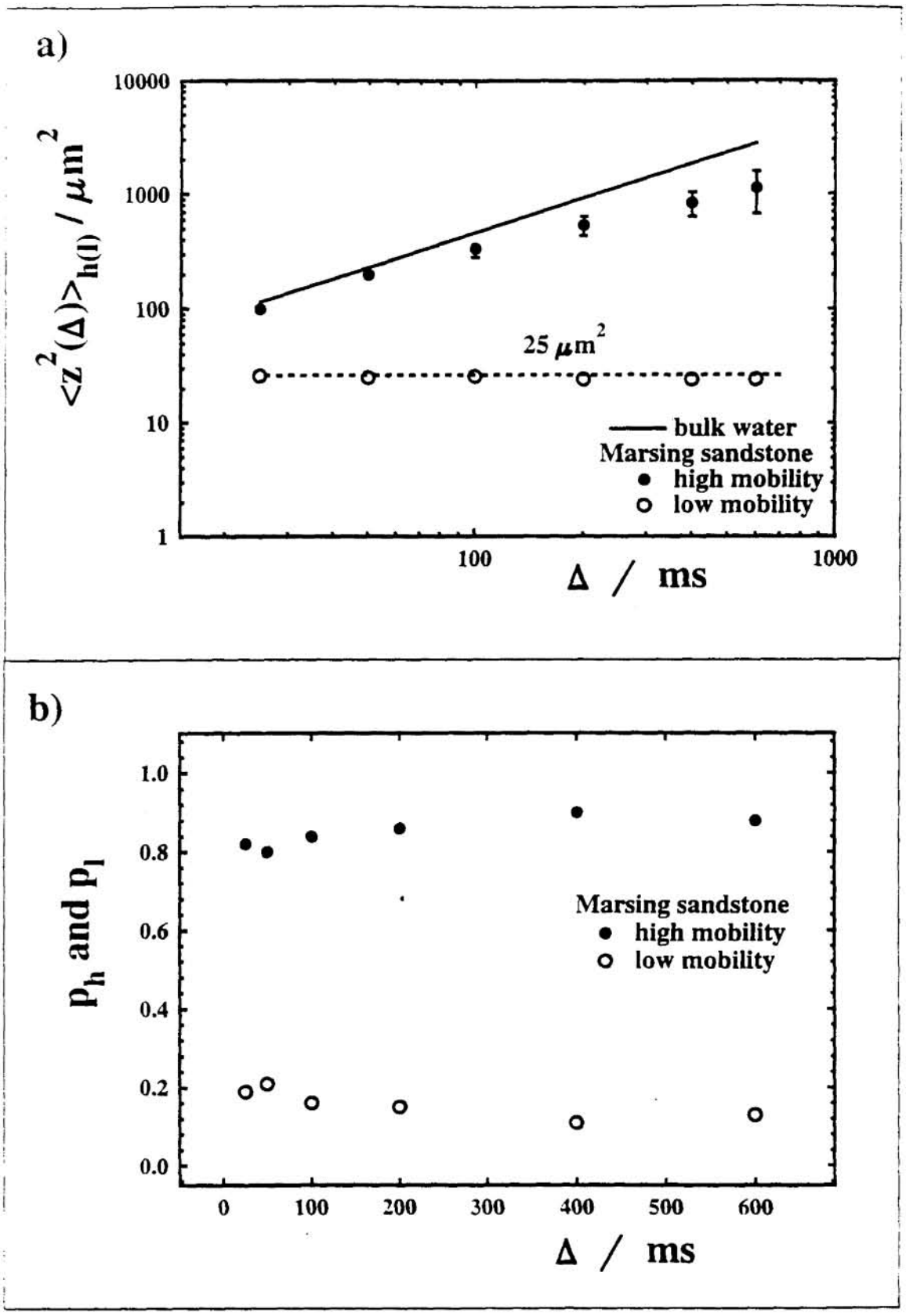
a)
10000
1000
100
10
1
$<z^2(\Delta)>_{h(l)} / \mu m^2$
25 μm^2
bulk water
Marsing sandstone
high mobility
low mobility
100
1000
Δ / ms
b)
1.0
0.8
0.6
0.4
0.2
0.0
p_h and p_l
Marsing sandstone
high mobility
low mobility
0
100
200
300
400
500
600
Δ / ms

Fig. 3